Macromolecules

Subscriber access provided by POSTECH Library

Article

Reinforcement of Amorphous and Semicrystalline Polymer Interfaces via in-Situ Reactive Compatibilization

Kilwon Cho, and Fengkui Li

Macromolecules, **1998**, 31 (21), 7495-7505 • DOI: 10.1021/ma971019y

Downloaded from http://pubs.acs.org on November 28, 2008

More About This Article

Additional resources and features associated with this article are available within the HTML version:

- Supporting Information
- Links to the 4 articles that cite this article, as of the time of this article download
- Access to high resolution figures
- Links to articles and content related to this article
- Copyright permission to reproduce figures and/or text from this article

View the Full Text HTML

ACS Publications
High quality. High impact.

Macromolecules is published by the American Chemical Society. 1155 Sixteenth Street N.W., Washington, DC 20036

Reinforcement of Amorphous and Semicrystalline Polymer Interfaces via in-Situ Reactive Compatibilization

Kilwon Cho* and Fengkui Li

Department of Chemical Engineering and Polymer Research Institute, Center for Advanced Functional Polymers, Pohang University of Science and Technology, Pohang 790-784, Korea

Received July 10, 1997; Revised Manuscript Received March 23, 1998

ABSTRACT: The interfacial reinforcement between polypropylene (PP) and amorphous polyamide (aPA) has been investigated by in-situ reactive compatibilization. PP reactivity with aPA was introduced by melt blending a certain amount of maleic anhydride grafted polypropylene (mPP) with pure PP. The effects of the mPP content, bonding time, and temperature on the interfacial fracture toughness, G_C, of the aPA/(PP + mPP) adhesive joint were studied. The G_C values were measured by means of a wedge test in an asymmetric double cantilever beam geometry. The G_C enhancement was proved to be due to the in-situ formation of copolymers at the interface by the use of contact angle measurements and X-ray photoelectron spectroscopy (XPS) analysis. Incorporation of 3 wt % mPP in the mixed PP would be enough for effective interfacial reinforcement in this particular system. At a certain bonding temperature, the interfacial fracture toughness reaches the saturation value G_C* above the critical bonding time. The value of G_C* increases, but *not* monotonically, with critical areal density of copolymers at the interface Σ_C as a result of increased bonding temperature. The effect of bonding temperature on the G_C* can be divided into three distinct temperature regions: (i) a region below the glass transition temperature of aPA and the beginning temperature of melting of mixed PP where there is virtually no adhesion; (ii) a region across the melting range of mixed PP crystals where the interfacial fracture toughness steadily increases with temperature; (iii) a region well above the melting temperature of mixed PP where G_C becomes relatively low. Scanning electron microscopy (SEM) and XPS results show that fibrillation of PP induced by the interfacial adhesion and subsequent breakage of the fibrils are the characteristics of fracture mechanism. Due to different crystalline morphologies of PP at different bonding temperatures, fracture mechanisms phenomenologically vary with bonding temperature at the microscale. Analysis on the locus of failure by microscopy and XPS reveals that the interfacial fracture toughness G_C of amorphous and semicrystalline polymer pairs in the reactive system is influenced not only by the areal density of copolymers formed at the interface but also by the crystalline morphology of the system.

Introduction

Interfacial adhesion plays an important role in the mechanical properties of polymer blends. However, most of the polymer pairs are thermodynamically immiscible. Therefore, the interfacial fracture strength is very weak due to there not being enough interdiffusion of molecules to create entanglements on both sides of the interface.[1]

A lot of studies have been performed on the use of reactive interfacial agents to improve the interfacial properties and control the morphologies of polymer blends. The reactive interfacial agents have specific functional groups and are able to generate in-situ formation of block or graft copolymers at the interface during the blend preparation through the reaction of functional groups incorporated onto the blend components.[2,3] Reactive compatibilization has been proved to be an effective means for morphology control in a variety of blend systems.[4−7] However, the fundamental understanding of the enhancement of interfacial adhesion resulting from reactive compatibilization is relatively limited.[8−13]

Recently, some works have been reported on the studies of polymer interfaces by reactive compatibilization. Most of them are focused on amorphous polymer pairs.[14−17] Lee and Char[14] reported that interfacial adhesion between an immiscible amorphous polyamide and polystyrene was enhanced by the addition of thin layers of styrene−maleic anhydride (SMA) random copolymer. The remarkable increase of fracture toughness of the interface over a certain interfacial region was explained to result from a certain interfacial region in which the diffusion and reaction are comparable. Briber and co-workers[15] investigated the effect of sulfonated polystyrene on the adhesion between immiscible polystyrene and poly(2-vinylpyridine) interface by varying the concentration of sulfonic acids of sulfonated polystyrene. The optimum concentration for interfacial reinforcement between the two immiscible polymer pairs was observed. Furthermore, Kramer and coworkers[16] reported an elegant set of experiments on the reinforcement of the polymer interface between the polystyrene and epoxy resin using end-functionalized polystyrene of different molecular weights which can be end-grafted into an epoxy network during curing. The effects of the interlinking chain length and grafting density on fracture toughness of the polystyrene/epoxy interface were elucidated. In a previous paper,[17] we reported our studies on the enhancement of interfacial adhesion between polystyrene and SMA via reactive reinforcement using amine-terminated polystyrene (ω-amino-PS) as a reactive compatibilizer. The enhancement of fracture toughness is evaluated as a function of molecular weight and content of ω-amino-PS, i.e. interlinking chain length and areal density of the interlinking molecules.

* To whom all correspondence should be addressed. Tel: +82-562-279-2270. Fax: +82-562-279-2699. E-mail: kwcho@postech.ac.kr.

10.1021/ma971019y CCC: $15.00 © 1998 American Chemical Society
Published on Web 10/02/1998

However, most of the studies are concerned with amorphous polymer pairs. Basic studies on the reactive reinforcement of the interface in semicrystalline polymer pairs are very limited. Until very recently, two studies have been reported.[18,19] Manson and co-workers[18] studied the fusion bonding of maleic anhydride grafted polypropylene to polyamide 6 via in-situ block copolymer formation at the interface. The interfacial fracture toughness was found to increase with the bonding temperatures. Optimal bonding required melting of both polymers and resulted in the highest fracture toughness which approached the value of cohesive fracture toughness of the polypropylene bulk. It was suggested that as crystallization proceeded each half of the in-situ-formed block copolymer was incorporated into crystalline domains on their respective sides of the interface, therefore enhancing the interfacial fracture strength. Around the same time, Leger and co-workers[19] reported their results on the same system but focused on the relationship between the interfacial fracture toughness and the areal density of copolymers at the interface. The interfacial fracture toughness was found to vary as the square of the areal density of copolymers at the interface, a relationship similar to that observed and predicted for glassy polymers. The common characteristic of the above two studies, however, can be summarized as the sole effect of chemical structure, i.e. the formation of copolymers on fracture toughness at the interface. More complicated mechanics of failure made it difficult for a more in-depth understanding of the fracture mechanisms in this system. In fact, in semicrystalline polymer systems, not only the areal density of block copolymers at the interface but also the morphology of each plate will play important roles in determining the interfacial properties. The study of polymer pairs, in which one is semicrystalline and the other is amorphous, may provide a good system for investigating the role of crystalline morphology on the interfacial adhesion because this system is simpler than semicrystalline polymer pairs. This information has not been available in the literature.

So, in this paper, we focus on the system of crystalline polypropylene and amorphous polyamide. Reactivity is introduced into the system via mixing a certain amount of maleated polypropylene, MAH-*g*-PP, with the pure PP. The objectives of this paper are (i) to investigate the effect of in-situ compatibilization such as the areal density of copolymers at the interface symbol $\sum$ on the interfacial properties in this particular system and (ii) evaluate the role of crystalline morphologies in the enhancement of interfacial fracture toughness at the interface. The relationships between the fracture mechanism and the structure across the interface are also investigated.

Experimental Section

Materials. Polypropylene (PP) used in this study is commercial mold grade Daelim Poly PP, supplied by Daelim Industrial Co., Ltd. The powderlike maleic anhydride grafted PP (m-PP) was obtained from Honam Petrochemical Co. Its melt index MI is 2000 g/10 min at 230 °C (ASTM: D 1238). The MAH content was determined to be 2.91×10^{-4} mol/g by titration. Amorphous polyamide (aPA) is CX-3000, obtained from Unitika Co. Solvents such as *N*,*N*′-dimethylformamide and acetone were directly used as received.

Sample Preparation. Mixtures of PP and mPP powder were melt blended in a Brabender internal mixer at 190 °C for 10 min. The aPA granules were dried in a vacuum at 100 °C for 24 h prior to use. Plaques for the bonding experiments were made by compression molding for 10 min at 190 and 220 °C for mixed PP and aPA, respectively. They were then cooled to room temperature by running water under the pressure. The mold dimension was approximately $50 \times 50 \times 2$ mm. To obtain smooth and clean molding surfaces, a polished Ferrotype plate was used as a molding base. The molded sheets were kept in a vacuum oven and were made into bonded laminates within 24 h in order to avoid contamination.

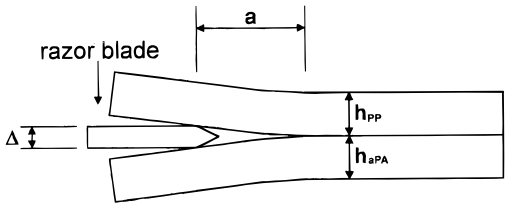

Figure 1. Schematic diagram of the fracture test geometry used to measure the interfacial fracture toughness G_C.

Bonding experiments were conducted by positioning the plaques of the mixed PP and aPA into contact under light pressure in a temperature-controlled compression molder. If not specified, the specimens were cooled slowly at a rate of about 1 °C/min after a certain bonding time in order to eliminate the residual stress. The bonded specimens were cut into strips of 5 mm in width using a diamond saw and then kept at ambient temperature for 2 days before the measurements of fracture toughness.

Measurements of Interfacial Fracture Toughnesses. Interfacial fracture toughnesses, G_C, were measured using an asymmetric double cantilever beam test. The crack was initiated by inserting a razor blade into the mixed PP/aPA interface. It was allowed to propagate slowly for 24 h before measurement. Due to the transparency of the polyamide plaque, the crack length was able to be measured by a traveling microscope. The schematic drawing of the geometry and parameters used in the test is shown in Figure 1. The interfacial fracture toughnesses, G_C, were then calculated according to the relation

$$G_C = \frac{3}{8}\frac{\Delta^2 E_{PP} h^3_{PP} E_{aPA} h^3_{aPa}}{a^4}\frac{E_{PP} h^3_{PP} C^2_{aPA} + E_{aPA} h^3_{aPA} C^2_{PP}}{(E_{PP} h^3_{PP} C^3_{aPA} + E_{aPA} h^3_{aPA} C^3_{PP})^2} \quad (1)$$

where Δ is the thickness of the razor blade, a is the crack length ahead of the blade, E_i and h_i denote the Young's modulus and the thickness of material i, respectively, and $C_i = 1 + 0.64\ h_i/a$.[6,20,21] The thickness ratio over a wide range was found to have a significant effect on the interfacial fracture toughness determination in glassy[20,22−23] and semicrystalline polymer pairs.[19] However, in this system, pre-experiments have shown that the ratio has not much effect when it ranges from 0.45 to 0.7 (Figure 2). Despite this, the mixed PP plate thickness was deliberately increased slightly more than that of the polyamide, to induce the crack to propagate along the PP/aPA interface.[20−24]

Due to the different thermal expansion coefficients of the two materials, adhesive joints were slightly bent when the cooling rate was relatively fast after bonding. In general, the volume variation of amorphous polyamide is almost negligible while that of polypropylene is able to reach as high as 5−10%. So, to obtain reliable results, the residual stress effect should be minimized during bonding experiments.

Figure 3 gives the results of interfacial fracture toughness for different cooling rates while their bonding conditions are kept constant on purpose. When the bonded samples are allowed to slowly cool at the rate of about 1 °C/min, the interfacial fracture toughness is able to reach as high as 70 J/m^2. However, the interfacial fracture toughness becomes sharply decreased even when the cooling rate is just more than 10 °C/min. The bonded specimens phenomenologically appear

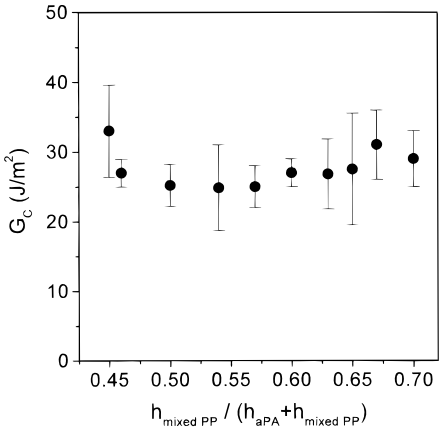

Figure 2. Interfacial fracture toughness G_c as a function of the aPA to mixed PP sheet thickness ratio for an aPA/mixed PP adhesive joint.

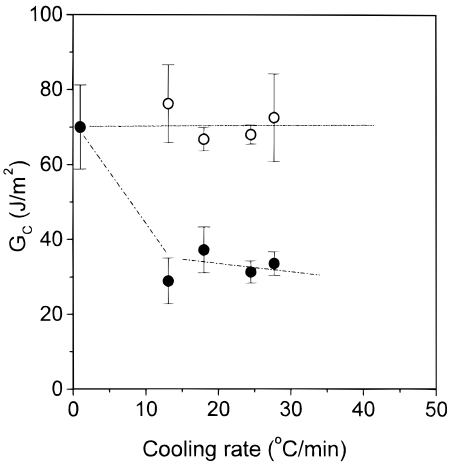

Figure 3. Interfacial fracture toughness G_C as a function of cooling rate for the specimens containing 3 wt % mPP bonded at 166 °C for 2.5 h: ●, prepared at different cooling rate; ○, remelted and subsequent cooled at the rate of 1 °C/min for the corresponding specimens. mPP content: 3 wt %.

a little bent in that case. So, the decrease of interfacial fracture toughness is attributed to the residual stress of the bent specimens. If these samples were reannealed at 166 °C for just an additional 5 min, and then followed by slowly cooling at 1 °C/min, the interfacial fracture toughness would increase and reach the normal value as shown in Figure 3. Therefore, residual stresses can be minimized by controlling the cooling rate. The fluctuation of the G_C values of the reannealed sample is probably due to the multiple-step treatments in the reannealing process.

Characterization of Areal Density of Copolymers at the Interface. To determine the areal density of copolymers formed at the interface, the unreacted aPA was dissolved out by DMF in the uncleaved section of a sample. DMF is a good solvent of aPA but cannot swell PP. The majority of the polyamide material, i.e., the unreacted polyamide in the uncleaved section of a sample, was removed. However, the reacted polyamide molecules were not able to be washed out due to their covalent bonding to mPP chains at the interface. The DMF-treated surface was then washed by surplus acetone for several times to extract any DMF molecules that may have possibly adhered to the surface. The specimen was then vacuum-dried and kept in the desiccator. The solvent-treated PP surface was analyzed by contact angle technique. Contact angle measurements were employed to obtain indirect determination of areal density of copolymers at the interface. They were conducted in a contact-angle meter (Kyowa Kaimenkagaku Co. Ltd) at room temperature, using distilled water as a contact media. One result was obtained by averaging at least five respective points.

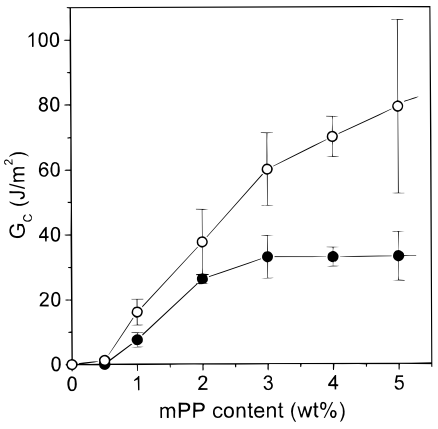

Figure 4. Interfacial fracture toughness G_C as a function of mPP content in mixed PP: ●, 166 °C/1 h; ○, 166 °C/2 h.

Examinations of Fracture Surfaces. To study the failure mode and locus of failure, the fracture surfaces were examined by scanning electron microscopy (SEM, JEOL JSM-6300F). The samples were coated with gold. The transsectioned photographs for the cleaved specimens were taken by optical microscope (Zeiss Axioplan) in a polarized transmission mode. For this purpose, a section, thin enough to transmit light, was produced using the polishing technique.

Chemical analysis on the fractured surfaces was conducted on the X-ray photoelectron spectroscope (XPS, Kratos XSAM800pci) using a Mg Kα source ($h\nu$ = 1253.6 eV). The spectra were collected at a takeoff angle between the sample and the detector of 15° for the 1s peaks of carbon, nitrogen, and oxygen near 285, 400, and 530 eV, respectively. Three spots were randomly selected for averaging the data. The atomic concentrations of each element were calculated using the sensitivity factors of 0.25 (carbon), 0.42 (nitrogen), and 0.66 (oxygen).[25]

DSC Measurements. DSC measurements were made on a Perkin-Elmer DSC-7 thermal system purged with nitrogen. Its temperature scale was calibrated from the melting characteristics of indium. The heating rate is 10 °C/min, at which the recrystallization effect may be negligible. The sample weight was about 10 mg. All curves were normalized to the unit weight of the sample.

Results and Discussion

Effect of mPP Content on the Interfacial Fracture Toughness. The anhydride group of mPP can react with the amine end-group of aPA and form in-situ graft copolymers containing imide linkage at the aPA/PP interface.[26] The enhancement of interfacial fracture toughness between mixed PP and aPA is, therefore, expected to be due to the in-situ formation of copolymers. In the case of pure PP, no well-bonded specimen survived even when the bonding temperature was much higher than the melting point of PP, implying that interfacial fracture toughness between pure PP and aPA is very low. PP and aPA are, therefore, thermodynamically immiscible.

However, when a certain amount of mPP is mixed with pure PP, the reactivity with aPA can be introduced into the system. Figure 4 shows the effect of mPP concentrations on the interfacial fracture toughness between mixed PP and aPA. The bonding temperature was set to be 166 °C, which is well above the glass transition temperature of aPA and on the verge of the melting peak of mixed PP. It shows that a very small amount of mPP, 0.5 wt %, does not result in good adhesion strength even at the bonding time of 2 h. As the mPP concentration increases, the interfacial fracture

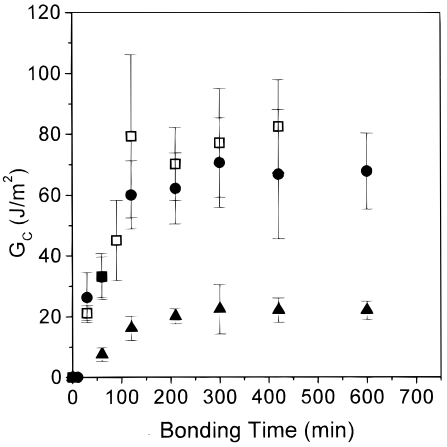

Figure 5. Interfacial fracture toughness G_C as a function of bonding time for the aPA/(PP + mPP) adhesive joint wih different mPP content: ▲, 1 wt %; ●, 3 wt %; □, 5 wt % mPP. Bonding temperature: 166 °C.

toughness is enhanced. After the mPP content reaches 3 wt %, the interfacial fracture toughness becomes slightly leveled off. It follows that the enhancement of interfacial adhesion between mixed PP and aPA is due to the in-situ formation of copolymers at the interface.

By variation of the bonding time, Figure 5 gives the detailed effects of the mPP content on the interfacial fracture toughness. For each series, interfacial fracture toughness increases with bonding time and then reaches a saturation value G_C*. The interfacial fracture toughness for 1 wt % mPP specimens is very low, while those of 3 and 5 wt % mPP specimens have higher values and are nearly overlapped. Generally, less than 5 wt % functional polymers are often used for the reactive compatibilization in immiscible polymer blends.[27] Our results show that 3 wt % of mPP would be enough for the enhancement of the interfacial adhesion in this system.

Amine end groups of polyamide and maleic anhydride grafted polyolefins are known to be able to easily react with each other to form covalent bonds during processing.[27] The chemical reactions occurring at the interface of reactive blending of polymers are known to be under diffusion control, a consequence of the small translational diffusivity of macromolecules.[11,28] So, in the bonding experiments, diffusion of reactive species, i.e., mPP molecules in this system, from the bulk to the interface would control the in-situ reaction kinetics at the interface.

Recently, O'Shanghessy et al.[28] theoretically proposed that the critical density of in-situ-formed molecules at the interface Σ_C is dependent on the molecular weight, $\Sigma_C \sim N^{-0.5}$, in the ideal system where the pairs are in the molten state and have the same molecular weight N. When a critical surface coverage of diblock copolymer is attained, other reactive chains from the bulk cannot penetrate the barrier diblock copolymers; consequently, further reaction at the interface becomes exponentially small. Therefore, above the critical point the critical interfacial properties seem to have no relation with the concentrations of reactive molecules in the bulk. The appearance of saturated G_C* values with bonding time and the overlap of interfacial fracture toughness for the specimens with 3 and 5 wt % mPP are consistent with the predictions by O'Shanghessy et al.[28] In the case of 1 wt % mPP, much lower fracture toughness is obtained. This is attributed to inadequate

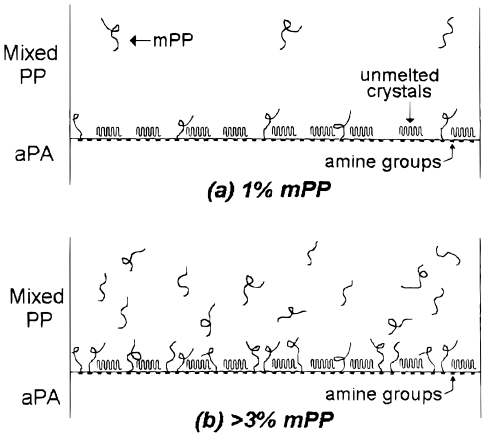

Figure 6. Schematic diagram of the models for the effect of mPP concentrations on the in-situ formation of copolymers at the interface.

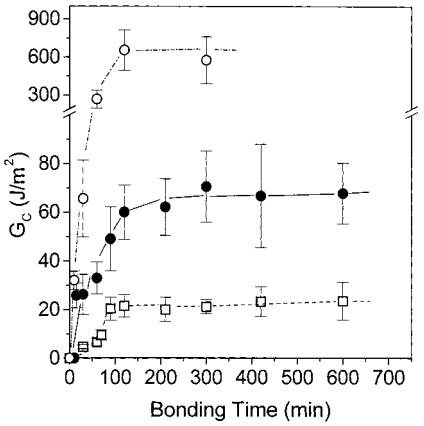

Figure 7. Interfacial fracture toughness G_C as a function of bonding time for the adhesive joint containing 3 wt % mPP at different bonding temperatures: □, 162 °C; ●, 166 °C; ○, 170 °C.

reactive molecules in the bulk of mixed PP. Figure 6 models the effect of functional molecule concentrations on the formation of copolymers at the interface. Thus, in the case of 1 wt % mPP, sufficiently high interfacial density, i.e., ideal saturation value, can never be reached by the diffusion controlled reactions. The *apparent* saturation interfacial fracture toughness in Figure 5 with time at this concentration corresponds to the point where the optimal amount of the anhydride groups has been consumed in the PP bulk near the interface. Due to the differences with the ideal system, it is difficult for the detailed theoretical evaluations in this particular polymer pair.

Effects of Bonding Time and Temperature. The dependence of interfacial fracture toughness G_C on the bonding time at different bonding temperatures is shown in Figure 7. At each temperature, the fracture toughness increases with bonding time and then reaches a saturation value G_C* at about 2 h. For each series, the cooling conditions are the same. So, at each bonding temperature, the enhancement of interfacial adhesion is mainly due to the increase of areal density of in-situ-formed copolymers at the interface. To determine the areal density of copolymers formed at the interface, the unreacted aPA molecules were dissolved out by DMF in the uncleaved section of the sample and then the remaining PP surface was analyzed by contact angle measurements. DMF is a good solvent of aPA but cannot swell the PP. Thus, after solvent treatment of

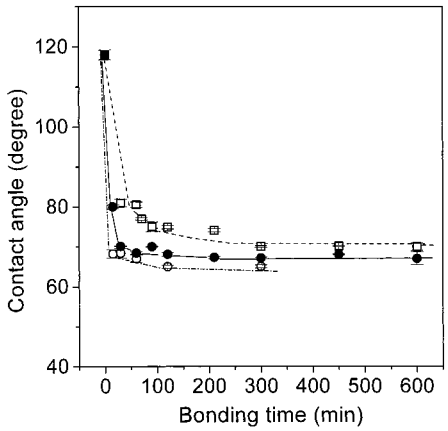

Figure 8. Contact angles of water on the solvent treated mixed PP surfaces for the specimens in Figure 7: □, 162 °C; ●, 166 °C; ○, 170 °C.

the adhesive joint, only the reacted aPA molecules remain on the top of the mixed PP surface. Contact angle is very sensitive to the composition of the top surface, and it has been a sensitive means for the surface characterization. Therefore, the results of contact angle indirectly represent the areal density of copolymers at the interface.

Figure 8 gives the contact angle results for all the samples in Figure 7 that were treated with a solvent. It shows that as the bonding time increases, the contact angles of water on the solvent-treated mixed PP surfaces decrease and then become constant after a certain time. Polypropylene is a hydrophobic polymer, so the interaction of water with its surface is very poor. Even in the case of 3 wt % mPP presence, it is still not enough to improve the wettability, and the contact angle of water on the prebonded mixed PP surface is as high as 118°. On the other hand, the abundance of hydrophilic groups along the backbone of aPA makes the contact angle much lower than that of mixed PP (63°). So, the decrease of the contact angle in Figure 8 indicates that more polyamide molecules appear on the solvent treated mixed PP surfaces, indirectly reflecting the increase of areal densities of copolymers at the interface. That is to say, at constant bonding temperature, the number of in-situ-formed copolymers at the interface increases with bonding time. When the areal density is dense enough, i.e. critical areal density is reached, reactions will not occur near the interface due to the steric hindrance. This will be discussed in more detail in a later section.

Figure 7 also shows that the saturation fracture toughness G_C* increases with bonding temperatures. The critical areal densities of copolymers at the interface seem to increase with bonding temperature, as inferred by the results of contact angle. This seems contradictory to O'Shanghessy's predictions,[28] where the critical areal density of copolymer would not be affected by temperatures if the pairs were totally melted. However, it should be noticed that different conditions such as crystalline morphology exist in our case. In this system, the dependence of saturation fracture toughness G_C* with bonding temperature is closely related to the crystalline morphology of the mixed PP. As shown by the DSC thermogram in Figure 12, different portions of mixed PP crystals melt at selected temperatures. The difference of the saturation interfacial fracture toughness for the three different temperatures shown in

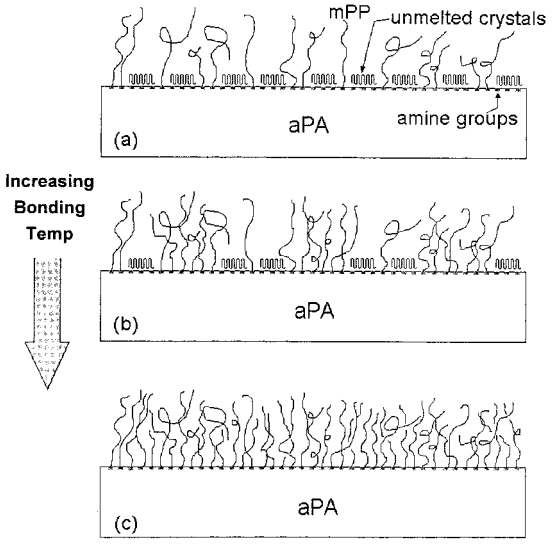

Figure 9. Schematic diagram of the formation of critical areal density of copolymers at the interface at various bonding temperatures. Bonding temperature increases from (a) to (c).

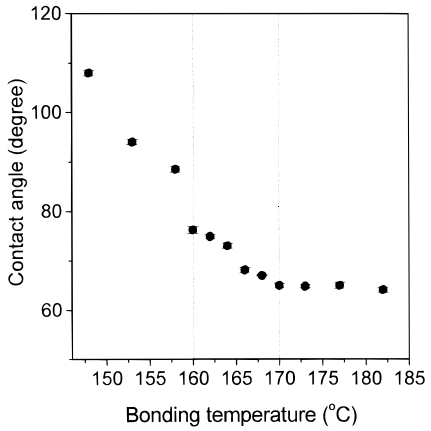

Figure 10. Contact angles of water on the solvent-treated mixed PP surfaces for the specimens in Figure 11.

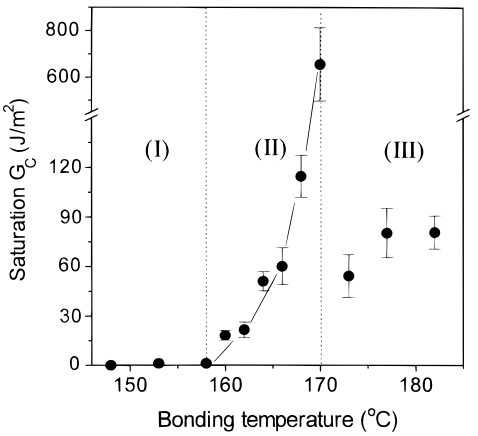

Figure 11. Saturation interfacial fracture toughness G_C* as a function of bonding temperature for the specimens containing 3 wt % mPP. Bonding time: 2 h.

Figure 7 may probably be due to the barrier effect of unmelted lamellar crystals on the diffusion of reactive mPP molecules to the interface.

Figure 9 schematically illustrates the effects of crystalline morphology of the mixed PP on the saturation areal density of in-situ-formed copolymers at the interface. At lower temperatures, many lamellar crystals

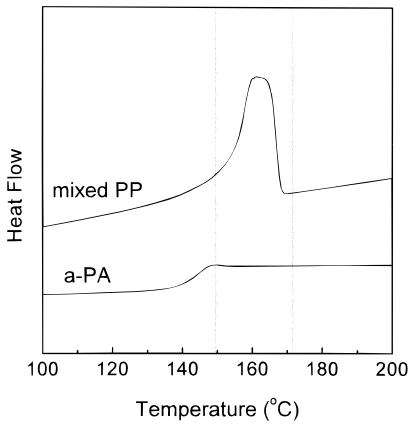

Figure 12. DSC thermograms of the mixed PP and aPA before bonding.

exist in an unmelted state near the interface. Therein, less dense coverage of copolymers would reach the critical value. As bonding temperature increases, the portion of unmelted lamellar crystals near the interface becomes small and further reaction between aPA and mPP molecules takes place, which makes it possible for the in-situ-formed copolymers to densely disperse across the interface. That is the reason the saturation interfacial fracture toughness increases with the bonding temperature within this temperature range. Accordingly, on the basis of this assumption, in the cases of totally melted specimens, i.e., above 170 °C, the critical areal density would not significantly change with the bonding temperature as O′Shanghessy[28] had theoretically expected. This will be discussed in the following section.

With such a problem it may be then asked why is the amount of time it takes to reach the critical areal density almost the same within this temperature range? At lower temperature, diffusion of functional molecules to the interface becomes low, but the extent of reactions needed to reach the saturation value is also low. On the other hand, at higher temperatures, although the diffusion rate increases, the number of functional groups necessary to reach the saturation limit is consequently high. The similar saturation time for different bonding temperatures as shown in Figure 7 is therefore due to the fact that diffusion and reactions of functional molecules near the interface are comparable at each bonding temperature.

The interfacial properties are subsequently investigated over the entire temperature range for the samples with 3 wt % mPP. The bonding time of 2 h is selected in order to reach the saturation fracture toughness G_C* at each temperature. Figure 10 shows the contact angles of water on the solvent-treated mixed PP surfaces for the specimens bonded at various temperatures for 2 h. A monotonic decrease of contact angles is obtained over the temperature range, indirectly indicating that critical areal density of copolymers at the interface increases with bonding temperature. (Note that the contact angles of water on mixed PP and aPA are about 118 and 63°, respectively.) The leveling off of the contact angles above the melting temperature of mixed PP shows that the critical interfacial property becomes constant after crystals of mixed PP totally melt, indicating the validity of our assumption as discussed above.

From the viewpoint of areal density, the saturation fracture toughness G_C* should monotonically increase with bonding temperature,[19,29−32] $G_C \sim \Sigma_C^n$, where Σ_C is the corresponding critical areal density of copolymers at the interface and n is a positive constant. However, unexpected results have been obtained for the relationship between saturation G_C* and bonding temperatures as shown in Figure 11. It seems that, generally, the higher the bonding temperature, the stronger the saturation interfacial fracture toughness G_C*. Furthermore, if we refer to the DSC thermograms of as-compression-molded mixed PP and aPA plaques in Figure 12, this trend can be divided into three distinct temperature regions: (I) a region below the glass transition temperature of aPA and the starting point of polypropylene melting temperature T_s where there is virtually no adhesion (the samples were completely delaminated before the interfacial fracture toughness could be measured); (II) a region across the melting zone of the mixed PP where the saturation fracture toughness G_C* increases with bonding temperature and reaches a maximum at T_e; (III) a region well above the melting of mixed PP crystals where saturation G_C* becomes relatively low.

In region I, polypropylene is semicrystalline solid, while amorphous polyamide is in the glassy state. So, no bonding would be expected. Some reactions between the two functional groups at the interface may not be completely precluded. However, the contact areas for two solid polymer materials are so limited that only a very small portion of these groups possibly participates in the reaction across the interface, which is far too inadequate for the adhesion of two-layer plaques.

In region II, there is a steady increase in the saturation G_C* values. In this region the polypropylene is partially melted and the polymer chains are now able to diffuse. The anhydride functionalized polypropylene is polar and may diffuse to the mixed PP/aPA interface. The driving force for the migration of functional segments to the interface is the reduction in surface energy. Polyamide is in the rubbery state within this temperature range. Because of the abundance of amine groups near the interface, the reaction kinetics is mainly controlled by the diffusion of anhydride groups to the interface from the bulk of mixed PP. With the increase of bonding temperature, more and more crystals melt. Elimination of the barrier effect of the unmelted lamellas with the increase of bonding temperature enhances the critical areal density of copolymers at the interface. This has been discussed above and illustrated schematically in Figure 9. Of course, the sudden increase of interfacial fracture toughness G_C* at T_e = 170 °C is unexpected. This is virtually due to the cohesive fracture, rather than adhesive one, and will be discussed later.

In region III, polyamide molecules become more mobile, while all the polypropylene molecules are in the molten state. In this region, the reaction rate across the interface is expected to be much faster than those at lower temperatures. The contact angles have also indirectly shown high critical areal densities in this temperature region (Figure 10). However, it is surprising to see that the interfacial fracture energies G_C* are lower than those of 168 and 170 °C and are of the same magnitude compared with those specimens at other lower temperatures.

The results shown in Figure 11 are qualitatively similar to the relationship between bonding temperatures and G_C found by Lee and Char[14] and the relation-

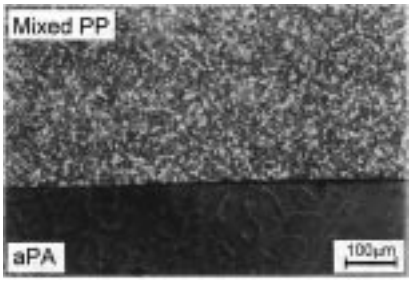

Figure 13. Trans-sectioned polarized optical micrograph of the interface region for the aPA/mixed PP adhesive joint prepared at 166 °C for 2 h. The dark line represents the crack.

ship between reactivity and G_C found by Beck Tan et al.[15] In Char's paper,[14] the sample preparation is quite different from ours. The reactive compatibilizer SMA was dissolved into toluene and then was spun onto the aPA sheet. The thickness of the reactive SMA layer is only 30 nm at the interface between PS and aPA. So, there may exist a competition between the reactivity at the interface and the diffusion of SMA molecules to the PS phase to form entanglements with bulk PS molecules during the bonding process. However, in our case, functional molecules were mixed together with bulk PP, so the whole process is a diffusion-controlled reaction. Beck Tan et al.[15] employed polymers with various functionality to study the relationship between the reactivity and G_C. However, in this work the same type and amount of functional molecules have been used. It is expected that reactivity at the interface will not be influenced much by varying bonding temperatures within this temperature range. Furthermore, after bonding, the samples underwent a 1-grade phase transition, i.e., from melt to crystalline state, in our experiments. This is quite different from the glass transitions in the above two cases. So, there are no similarities between their results and ours, and their explanations cannot be suitable for interpreting the results shown in Figure 11.

Generally, the enhancement of interfacial fracture strength is mainly due to the in-situ copolymer formation at the interface, while some other factors, for example crystalline morphology, must also play an important role in the subdivisions of three distinct temperature regions. To elucidate this irregular temperature dependence of saturation fracture toughness, analysis of the fracture mechanisms becomes necessary.

Fracture Mechanisms. Since the yield stress of polypropylene is much lower than that of amorphous polyamide, the crack tends to propagate in the bulk of the material with lower yield stress, i.e., polypropylene when the interface is strong. The locus of failure was analyzed by various techniques such as microscopic examination and XPS analysis. The results will be discussed in more detail in the following section. Figure 13 shows the typical trans-sectioned polarized optical micrograph of the cleaved adhesive joint specimen. It is clear that the fracture occurs very near the interface. However, unlike the amorphous polymer pairs, various fracture mechanisms are observed with the bonding temperature, in this case.

Figure 14 shows the SEM micrographs of the fracture surface of the polyamide side for a series of typical specimens over the temperature range. Figure 14a,a′ shows the SEM micrographs of the fracture surface of the polyamide side for the specimen prepared at 162 °C with different magnifications. At this low bonding

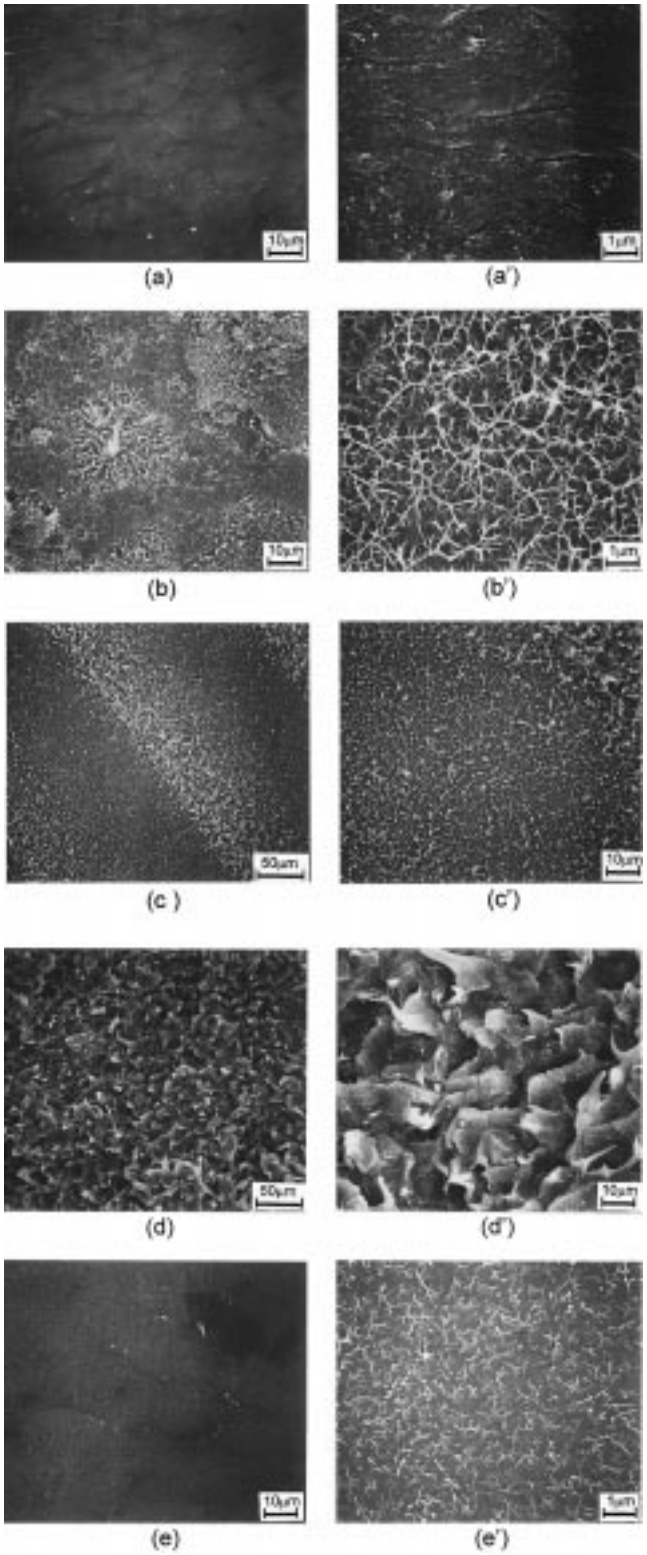

Figure 14. Scanning electron micrographs of the fracture surfaces of aPA for the aPA/mixed PP adhesive joints prepared at different bonding temperatures: (a, a′) 162 °C; (b, b′) 166 °C; (c, c′) 168 °C; (d, d′) 170 °C; (e, e′) 180 °C. Bonding time: 2 h.

temperature, the polypropylene partially melts, and only a small amount of maleic anhydride would participate in the reactions. The critical areal density of the copolymers formed at the interface is very low, which is clear from the results of the contact angle in Figure 10. This areal density might be enough to build up some stress at the crack tip during the crack propagation.

However, the stress at the crack tip is too small to induce plastic deformation of PP, i.e., the formation of large fibrils, which results in fairly low fracture toughness and a smooth fracture surface. Since the mPP used in this study has the molecular weight much higher than the critical value for effective chain entanglements, the fracture mechanism is expected to be chain scissions due to high frictional force on both sides. It should be noted that spherulitic patterns on the fractured polyamide surface in Figure 14a is attributed to the so-called "stamp effect". No evidence of significant plastic deformation of polypropylene is observed at high magnification (Figure 14a′).

As the critical areal density increases, the stress developed at the crack tip is able to approach the critical value for the formation of large fibrils in the material of lower yield stress, i.e. polypropylene in this case. Chain scissions along the fibrils will then follow, which leads to increased energy dissipation. Figure 14b,b′ shows the SEM micrographs of the fractured polyamide surface for the specimen prepared at 166 °C. Highly deformed polypropylene fibrils are observed. The average diameter of the fibrils is about 60 nm, i.e., a combination of several lamellas. The characteristic of this fracture pattern is layers of evenly deformed polypropylene fibrils dispersed by some spherulitic thick deformed polypropylene zones. Of course, the appearance of a large amount of deformed polypropylene fibrils is caused by an increase of the areal density of copolymers interlinking the two sides across the interface.

Figure 14c,c′ shows the SEM micrographs for the specimen prepared at 168 °C with higher critical areal density of copolymer at the interface. The spherulitic deformed pattern disappears. The crack tends to propagate toward the bulk of polypropylene, and then following fibril failure it returns back to the place near the interface again, resulting in the so-called "stick-slip" pattern. Periodic "stick-slip" failures are characteristic of this specimen. Similar features have been found in some amorphous polymer pairs.[21−24] This will be discussed in detail in the following section. As the critical areal density further increases, for example in the case of the specimen bonded at 170 °C, this periodicity disappears and complete cohesive failure is observed (Figure 14d,d′). Sharp increase of interfacial toughness is, therefore, expected.

At a much higher temperature, e.g. 180 °C, in which all the mixed PP crystals melt, the critical areal density becomes constant, but the saturation fracture toughness decreases, compared with those prepared at the temperatures slightly below 170 °C. The fracture surface is seemingly quite smooth as shown in Figure 14e. In high magnification (Figure 14e′), a very thin layer of polypropylene fibrils is found to evenly scatter on the polyamide surface, whose average diameter is much smaller than that in several of the former cases.

The same fracture surfaces were investigated by XPS in order to understand more precisely the path of the crack. The detected thickness was expected to be 10−15 Å. The main elemental difference between the two polymers is the presence of nitrogen in the amorphous polyamide. Table 1 lists the elemental compositions of fractured PP and aPA surfaces as measured by XPS. The values are the average compositions taken from three different spots. No nitrogen element was detected on the surfaces of fractured mixed PP. On the other hand, on the fracture surfaces of the selected aPA specimens, nitrogen was detected, showing that the crack propagated in the bulk of mixed PP but very near the interface. However, this result does not necessarily mean that the aPA fracture surface is covered by a layer of mixed PP fibrils less than 10−15Å in thickness. In fact, from the SEM photographs of the aPA side of the fracture surface as shown in Figure 14, the average diameter of mixed PP fibrils approximately reached as high as 50 Å. The detection of nitrogen element may be originated from the concave gaps among the fractured fibrils. Anyway, decrease of nitrogen on the fractured aPA surfaces as a function of bonding temperature can be related to the thickening of the covered PP fibril layers. The abrupt increase of nitrogen at higher temperature 180 °C means less PP fibril presence on the aPA surface after the fracture. This is consistent with the above SEM results.

Table 1. Elemental Compositions of Fractured aPA Surfaces Measured by XPS

	atomic concentration, %		
sample	N	C	O
	aPA		
calcd	7.3	85.4	7.3
as-molded	5.7 ± 0.3	78.1 ± 0.2	16.2 ± 0.5
162 °C/2h	1.4 ± 0.4	94.2 ± 1.3	4.4 ± 0.9
166 °C/2h	0.9 ± 0.3	97.3 ± 0.9	1.8 ± 0.6
170 °C/2h	0.3 ± 0.2	97.4 ± 1.5	2.4 ± 1.3
180 °C/2h	1.3 ± 0.7	96.4 ± 1.6	2.3 ± 0.9
	PP		
162 °C/2h	0	98.3 ± 0.3	1.7 ± 0.2
166 °C/2h	0	97.5 ± 0.6	2.5 ± 0.6
170 °C/2h	0	97.2 ± 0.2	2.8 ± 0.2
180 °C/2h	0	97.8 ± 0.5	2.2 ± 0.5

The elemental composition of the reference aPA does not have the expected ratio between oxygen and nitrogen. The oxygen is more abundant than nitrogen on the surface. This may probably be attributed to the adsorbed oxygen on the surface and the arrangement of the chemical groups on the surface by the steric hindrance of large aromatic units along the backbones of aPA.

Models on the Origination of Various Interfacial Fracture Mechanisms. But, how have various fracture mechanisms been originated at the monotonic increase of areal density of copolymers at the interface? This may be elucidated according to the phase separation models illustrated in Figure 15.

Baer and co-workers[33] have shown that in PP and mPP blends, phase segregation occurs when the mPP has a lower molecular weight and higher MAH content. The mPP tends to crystallize separately and form individual lamellar crystals. The number of "tie molecules" between PP and mPP lamellas drops very low. This has been indirectly verified by their peel test.

The mPP used in this study is very similar to that used by Baer et al. Unfortunately, because of only 3 wt % mPP presence in mixed PP, it is experimentally difficult to directly prove the existence of different lamellar crystals near the interface in this study. However, the DSC results for 50 wt % mPP specimens in Figure 16 do prove that phase separation occurs in this system. It is clear that PP and mPP have their individual melting points under the specified conditions. The appearance of one irregular melting peak between the two T_m's of PP and mPP for the as-blended sample indicates that most of PP and mPP molecules are able to cocrystallize in this case. When the blend is annealed

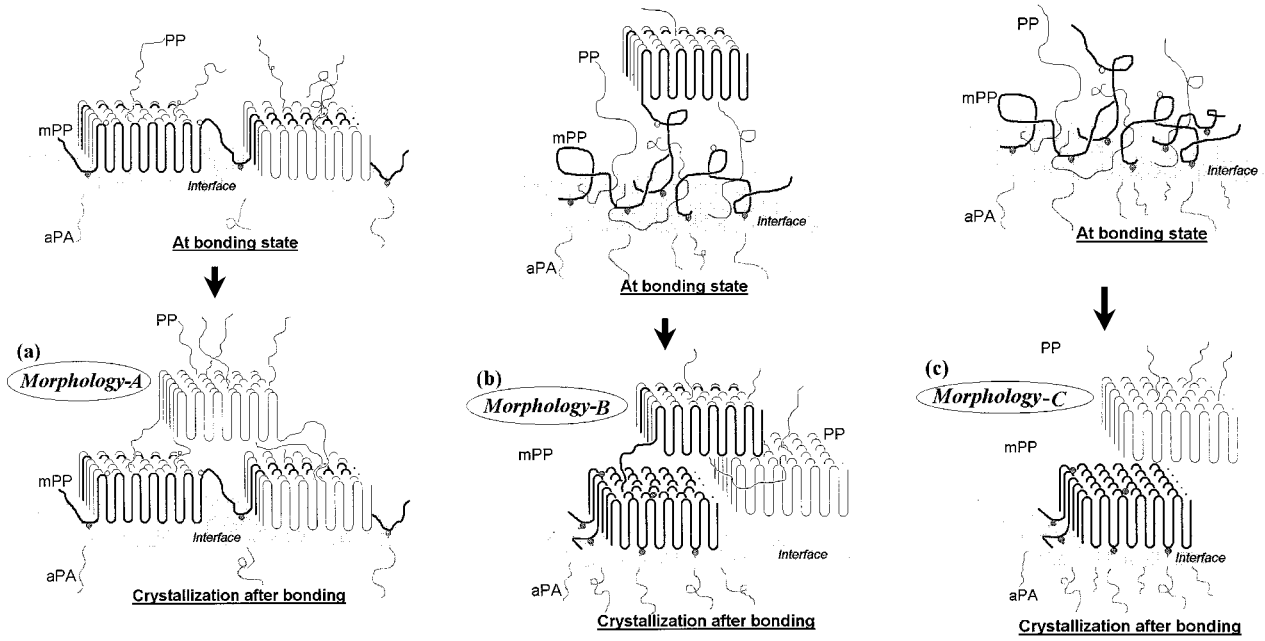

Figure 15. Schematic representation for the formation of various crystalline morphologies of mixed PP near the interface: (a) morphology A; (b) morphology B; (c) morphology C.

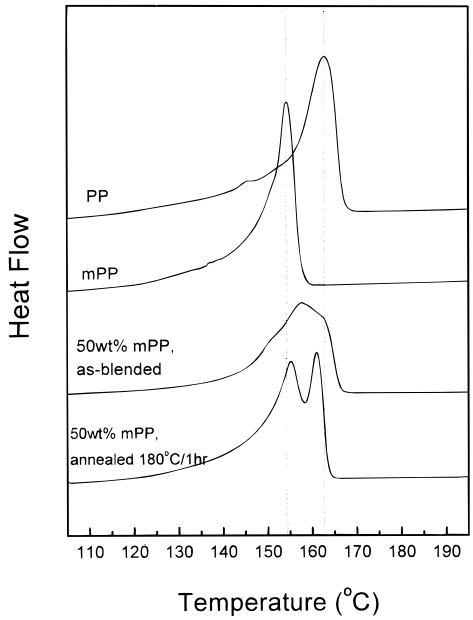

Figure 16. DSC thermograms of PP, mPP, and PP/mPP (50/50 wt %) blend under different preparation conditions.

at 180 °C for 1 h and subsequently cooled at a rate of 1 °C/min, which simulates the bonding conditions in this study, two distinct melting peaks appear, corresponding to the melting points of PP and mPP, respectively. The closing-up of them may probably be due to the overlap of the melting enthalpies of the two phases. Although the composition of mPP in Figure 16 does not match our case in this study, it does show that phase separation exists in our bonding experiments.

PP and mPP are able to be well mixed under shearing in the molten state. This is experimentally reasonable. Since the prebonded mixed PP plates were prepared by compression molding, and subsequently cooled rapidly by running water, it is possible for PP and mPP to cocrystallize during the cooling process. Thus, the as-molded mixed PP plates contain cocrystals before bonding experiments. This has been proved by the DSC results of Figure 16 for the mixed PP with the different composition. So, on the basis of the fact that the prebonded mixed PP plates are able to cocrystallize before the bonding experiment,[34] three different morphologies (morphologies^{A-C}) may exist near the interface in the *bonding* process.

Morphology A. At certain temperature range, mixed PP crystals partially melt. Some cocrystallized lamellar crystals may still exist at the interface while parts of those in the bulk nearby melt (Figure 15a). The mPP molecules trapped in these cocrystallized lamellas at the interface have enough mobility to diffuse and in situ react with aPA molecules on the other side. When the specimen is subsequently cooled at a very low rate, these lamellas near the interface are still able to tie in well with the as-crystallized lamellas in the bulk due to the abundance of pure PP molecules.

Morphology B. When mixed PP crystals partially melt, some originally cocrystallized lamellar crystals may melt at the interface while the lamellas in the bulk nearby may still exist in the form of cocrystal (Figure 15b). The melted mPP molecules at the interface have more freedom to react with the amine groups of aPA; meanwhile, those trapped in the unmelted cocrystallized lamellas off the interface inevitably diffuse and are covalently bonded with the aPA on the other side. As the temperature slowly decreases after bonding, the mPP and PP molecules tend to crystallize separately and form individual lamellas. A small amount of "tie molecules" still exists between the mPP lamellas at the interface and the cocrystallized lamellas in the bulk. But it is evidenced that the number of "tie molecules" will be lower than that in morphology A.

Morphology C. As the bonding temperature is well above the melting temperature of mixed PP, all the crystals of the mixed PP melt (Figure 15c). The mobility of mPP molecules will be very high. The mPP molecules both at the interface and from the bulk are able to react with amine groups of aPA on the other side. After bonding, as the temperature slowly decreases, due to the phase separation between PP and mPP, separate lamellas of PP and mPP tend to form. The connection

between the two different lamellas would be very weak. Since PP lamellas (97 wt %) dominate in the bulk, the tie molecules between the mPP lamellas at the interface and those of mPP off the interface would be negligible.

In a comparison of the three morphologies, the sequence for the interlamellar strength between those at and off the interfaces would be morphology A > morphology B > morphology C. If a crack proceeds along the interface, even at the same areal density of copolymer, stress produced at the crack tip should have the same sequence, i.e. morphology A > morphology B > morphology C. Different fibrillation would be expected from different morphologies after failure. So, various fracture mechanisms and irregular increase of interfacial fracture toughness with bonding temperatures can be interpreted as follows.

It is well-known that most of the mixed PP crystals exist in the form of spherulites in the bulk and, of course, on the surface as well. For the sample bonded at 162 °C for 2 h as shown in Figure 14a, the functional groups trapped in the vicinity of the lamellas are less mobile under this condition. Only a small portion of the mixed PP crystals melt, so reactions across the interface are quite limited. On the other hand, under this condition, aPA is just in the rubbery state. Due to the slight pressure in the bonding process, the soft surface of aPA is likely to be stamped by the still solidlike spherulites even though not enough chemical bonding exists between the mixed PP spherulites and the aPA surface. That is why at high magnification, as shown in Figure 14a′, no deformed mixed PP fibrils appear after fracture.

As bonding temperature increases, for example in the case of 166 °C, many imperfect crystals, i.e. small, and thinner lamellas melt. However, the temperature increase is still not enough to break up the whole spherulites on the surface. Thus, large spherulites still exist. In this case, reactions to form interlinking copolymers occur both in the melted interface area and in the partly melted spherulite zones. The value of the critical areal density of in-situ-formed copolymers is able to reach the critical point for the formation of mixed PP fibrils upon fracture at the interface. So, the characteristic of the fractured aPA surface is the covering of a mixed PP fibril layer as already shown in Figure 14b. The dispersion and protrusion of large spherulitic zones can be explained by the existence of different morphologies. In the melted interface region of mixed PP at the bonding temperature, morphology B is mainly obtained, while in the spherulitic zone at the interface, morphology A dominates. So, large fibrilled patterns appear on the layer of relatively small PP fibrils.

As the bonding temperature further increases, for example at 168 °C, most of the crystals will melt and spherulites may disappear. More reactions will occur at the interface, and the critical areal density of copolymers at the interface will accordingly increase as has been discussed in the previous section. In this case, periodic "stick-slip" failure is observed as shown in Figure 14c,c′. This "stick-slip" behavior may be partly due to the effect of the mixed mode of the stress state at the crack tip, i.e., the tensile and shear stress, which are affected by the modulus and thickness of each adherend of the adhesive joint.[20−24] The mixed mode of the stress state at the crack tip tends to deflect the crack toward the bulk of one of the adherends instead of propagating the crack along the interface. However,

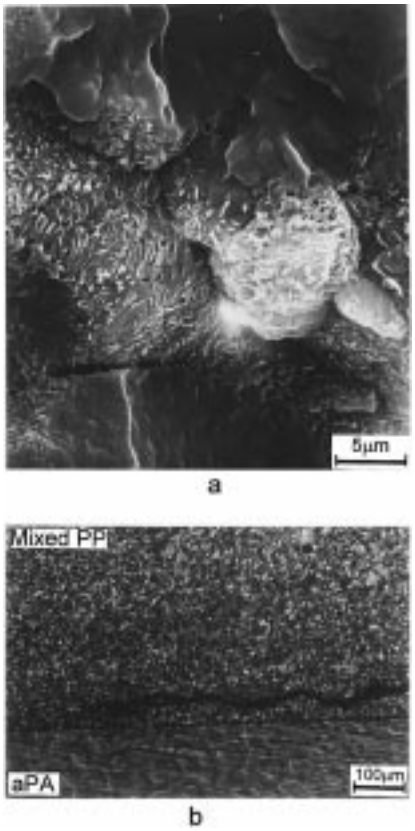

Figure 17. (a) Scanning electron micrograph of cryogenic fractured surface of mixed PP prepared at 170 °C for 2 h. (b) Trans-sectioned polarized optical micrograph of the interface region for the aPA/mixed PP adhesive joint prepared at 170 °C for 2 h. The dark line represents the crack.

our results have shown in Figure 2 that the effect of sample thickness ratios is not significant in this particular system. Furthermore, with the difference in the fracture mechanisms it should be noted that craze failure is characteristic for the previous amorphous interface[20−24] while fibrillation by plastic deformation is the predominant failure mode in this system. So, the "stick-slip" failure in this case does not seem to be attributed to the sole effect of the mixed mode of the stress state as in other amorphous systems. Noticeably, at this bonding temperature most of the mixed PP crystals melt, but small thicker lamellas still exist and statistically scatter in the bulk and at the interface. So, although the morphology B becomes dominant, morphology A still exists and fluctuates evenly around the interface. The crack tip has to meet both the "*weak*" and "*strong*" points periodically. This may be one of the possible reasons for this particular fracture mode in Figure 14c,c′.

At temperature 170 °C, at which all the mixed PP crystals just melt, the critical areal density of copolymers therefore increases. But, loosely packed mixed PP crystals are formed at this particular temperature (see Figure 17a). Once the crack is initiated toward the mixed PP bulk, it prefers to propagate along the so-called interspherulitic weaker path. This result in typical cohesive failure as is shown in Figure 17b, which causes the high saturation fracture toughness. However, the question of why does the special crystalline morphology form at this particular temperature still needs further studies.

As the bonding temperature is well above the melting of mixed PP (180 °C, for example), the mobility of mPP

molecules will be very high. The diffusion of mPP molecules and reactions at the interface will then occur much faster. Even though the critical areal density can be reached in a short time, other functional mPP molecules may continue to diffuse toward the interface. Of course, these molecules are no longer able to react with the aPA molecules due to the steric hindrance of the pre-reacted molecules, but they are able to make the mPP concentration relatively higher near the interface. After bonding, as the temperature slowly decreases, due to the phase separation between PP and mPP, morphology C is mainly obtained. So, even though the areal density of the copolymer at the interface is very high (Figure 10), only very thin fibrils are induced during interfacial fracture due to a relatively weak connection between the PP and mPP lamellar crystals. Herein, the interfacial fracture toughness therefore decreases and the fracture surface becomes smooth.

Conclusions

The interfacial fracture toughness G_C between amorphous polyamide and semicrystalline polypropylene can be enhanced via in-situ reactive compatibilization by the incorporation of maleic anhydride grafted polypropylene. The dependence of interfacial properties on the mPP content, bonding time, and temperature has been systematically investigated.

The interfacial fracture toughness is observed to reach the saturation value G_C* at a certain bonding time. The G_C* increases with critical areal density of copolymers at the interface as a result of increased bonding temperature but not monotonically. The interfacial property of amorphous and semicrystalline polymer pairs in a reactive system is influenced not only by the areal density of copolymers formed at the interface but also by the crystalline morphology of the system.

The crack propagates in the bulk of polypropylene but very near the interface. Fibrillation of mixed PP induced by the interfacial adhesion and subsequent breakage of the fibrils are generalized as the characteristics of the fracture mechanism. Due to different morphologies of PP at different bonding temperatures, fracture mechanisms phenomenologically vary at the microscale.

Acknowledgment. This work was supported by Non Directed Research Funds from the Korea Research Foundation (1996).

References and Notes

(1) Wool, R. P. In *Polymer Interfaces*: *Structure and Strength*; Carl Hanser Verlag: New York, 1995.
(2) Xanthos, M.; Dagli, S. S. *Polym. Eng. Sci.* **1991**, *31*, 929.
(3) Liu, N. C.; Baker, W. E. *Adv. Polym. Tech.* **1992**, *11*, 249.
(4) Koning, C.; Ikker, A.; Borggreve, R.; Leemans, L.; Moller, M. *Polymer* **1993**, *34*, 4410.
(5) Majumdar, B.; Keskkula, H.; Paul, D. R. *Polymer* **1994**, *35*, 3164.
(6) Beck Tan, N. C.; Tai, S.-K.; Briber, R. M. *Polymer* **1996**, *37*, 3509.
(7) Cho, K; Seo, K.H.; Ahn, T. O. *Polym. J.* **1997**, 29, 987.
(8) Fleischer, C. A.; Marales, A. R.; Koberstein, J. T. *Macromolecules* **1994**, *27*, 379.
(9) Yukioka, S.; Inoue, T. *Polymer* **1994**, *35*, 1182.
(10) Scott, C.; Macosko, C. *J. Polym. Sci., Part B: Polym. Phys.* **1994**, *32*, 205.
(11) Guegan, P.; Macosko, C. W.; Ishizone, T.; Hirao, A.; Nakahama, S. *Macromolecules* **1994**, *27*, 4993.
(12) Nakayama, A.; Inoue, T.; Guegan, P.; Macosko, C. W. *Polym. Prepr.* **1992**, *33* (2), 840.
(13) Cho, K.; Joen, H. K.; Park, C. E.; Kim, J.; Kim K. U. *Polymer* **1996**, *37*, 1117.
(14) Lee, Y.; Char, K. *Macromolecules* **1994**, *27*, 2603.
(15) Beck Tan, N. C.; Peiffer, D. G.; Briber, R. M. *Macromolecules* **1996**, *29*, 4969.
(16) Norton, L. J.; Smigolova, V.; Pralle, M. U.; Hubenko, A.; Dai, K. H.; Kramer, E. J.; Hahn, S.; Berglund, C.; DeKoven, B. *Macromolecules* **1995**, *28*, 1999.
(17) Cho, K.; Seo, K. H.; Ahn, T. O.; Kim, J.; Kim, K. U. *Polymer* **1997**, 38, 827.
(18) Bidaux, J.-E.; Smith, G. D.; Bernet, N.; Manson, J.-A. E.; Hilborn, J. *Polymer* **1996**, *37*, 1129.
(19) Boucher, E.; Folkers, J. P.; Hervet, H.; Leger, L.; Creton, C. *Macromolecules* **1996**, *29*, 774.
(20) Xiao, F.; Hui, C. Y.; Washiyama, J.; Kramer, E. J. *Macromolecules* **1994**, *27*, 4382.
(21) Brown, H. R. *J. Mater. Sci.* **1990**, *25*, 2791.
(22) Sikka, M.; Pellegrini, N. N.; Schmitt, E. A.; Winey, K. I. *Macromolecules* **1997**, *30*, 445.
(23) Brown, H. R. *MRS Bull.* **1996**, *21*, 24.
(24) Xiao, F.; Hui, C. Y.; Kramer, E. J. *J. Mater. Sci.* **1993**, *28*, 5620.
(25) Briggs, D.; Seah, M. P. In *Practical Surface Analysis, Vol. 1-Auger and X-ray Photoelectron Spectroscopy*, 2nd ed.; John Wiley & Sons: 1990; p 635.
(26) Ide, F.; Hasegawa, A. *J. Appl. Polym. Sci.* **1974,** *18*, 963.
(27) Xanthos, M. In *Reactive Extrusion, Principles and Practice*, Hanser Publishers: New York, 1992; p 139.
(28) O'Shaughnessy, B.; Sawhney, U. *Phy. Rev. Lett.* **1996**, *76*, 3444.
(29) Washiyama, J.; Kramer, E. J.; Creton, C. F.; Hui, C. Y. *Macromolecules* **1994**, *27*, 2019.
(30) Kramer, E. J.; Norton, L. J.; Dai, C. A.; Sha, Y.; Hui, C. Y. *Faraday Discuss.* **1994**, *98*, 31.
(31) Creton, C.; Kramer, E. J.; Hui, C. Y.; Brown, H. R. *Macromolecules* **1992**, *25*, 3075.
(32) Dai, C. A.; Jandt, K. D.; Iyengar, D. R.; Slack, N. L.; Dai, K. H.; Davidson, W. B.; Kramer, E. J.; Hui, C. Y. *Macromolecules* **1997**, *30*, 549.
(33) Duvall, J.; Sfllitti, C.; Myers, C.; Hiltner, A.; Baer, E. *J. Appl. Polym. Sci.* **1994**, *52*, 195; *52*, 207.
(34) Cho, K.; Li, F.; Choi, J. *Polymer*, in press.

MA971019Y